ATP-sensitive potassium channel and bursting in the pancreatic beta cell

A theoretical study

Joel Keizer and Gerhard Magnus
Institute of Theoretical Dynamics, and Department of Chemistry, University of California, Davis, California 95616

ABSTRACT Based on the existence of ATP-sensitive potassium channels in the plasma membrane of pancreatic beta cells, we develop a quantitative explanation of the electrical activity observed in pancreatic islets. The proposed mechanism involves the voltage-dependent inward calcium and outward potassium currents described by Rorsman and Trube (1986), which are voltage-activated when an increase in the cytoplasmic ATP/ADP ratio decreases the conductance of the ATP-sensitive potassium channels. It is proposed that modulation of the ATP/ADP ratio occurs through calcium inhibition of oxidative phosphorylation. In this picture the mitochondria serve as a transducer of metabolic activity whose sensitivity is modulated by cytosolic calcium. Solution of the differential equations that describe this mechanism gives rise to both bursting and continuous spiking electrical activity similar to that observed experimentally. While the mechanism for bursting in this model involves the ATP/ADP ratio, the feedback is still provided by calcium, as originally proposed by Chay and Keizer (1983) using a Ca^{2+}-activated potassium conductance. A mixed-model, which includes both ATP-sensitive and Ca^{2+}-activated potassium conductances, also reproduces the experimentally observed electrical activity and may correspond more closely to the actual situation *in vivo*.

I. INTRODUCTION

The pancreatic beta cell, when perfused with glucose in intact islets, exhibits a characteristic pattern of electrical activity called bursting. This phenomenon was discovered by Dean and Matthews (1970) using microelectrodes and has been the subject of intense experimental investigation in the intervening years (see Atwater et al., 1980, 1987 for recent reviews). Bursting consists of an active phase at a plasma membrane potential of ~ -25 mV, where rapid spikes of electrical activity are observed, and a silent phase at ~ -60 mV, where the potential rises very slowly. The silent phase alternates rhythmically with the active phase producing an overall period of the order of 15 s. The duration of the active phase has been shown to be related to the rate of glucose-stimulated insulin release in single islets (Meissner, 1976), and it is widely speculated that the uptake of Ca^{2+} that occurs during the active phase is involved in insulin granule exocytosis (Rubin, 1982; Wollheim and Sharp, 1981).

Several mechanisms have been proposed to explain bursting activity in the beta cell. Based on pharmacological evidence, Atwater, Rojas, and collaborators (Atwater et al., 1979 and 1980) proposed that a calcium-activated potassium conductance in the plasma membrane was responsible for switching the membrane potential between the depolarized active and hyperpolarized silent phase. In this picture, the active phase consists of rapid action-potential-like spikes involving an outward K^+ current and an inward Ca^{2+} current. Spiking causes Ca^{2+} to accumulate in the cytosol, and when the Ca^{2+} concentration is high enough, the Ca^{2+}-activated potassium conductance repolarizes the membrane, thereby shutting off the voltage-gated K^+ and Ca^{2+} currents that are responsible for the spiking activity. Ultimately, the slow, but perpetual, removal of Ca^{2+} from the cytosol depolarizes the plasma membrane to such an extent that the voltage-gated channels are reactivated and the cycle continues. Translating these ideas into a quantitative molecular mechanism, Chay and Keizer (1983) developed a so-called minimal model that explains many of the observed features of the glucose-induced electrical activity in the beta cell.

The molecular basis of this proposed mechanism was solidified by the discovery of Ca^{2+}-activated potassium channels in the plasma membrane of the beta cell (Cook et al., 1984) and by the documentation of voltage-regulated K^+ and Ca^{2+} conductances in the beta cell that are capable of supporting action-potential spikes near -25 mV (Rorsman and Trube, 1986). Unfortunately, while the unitary conductance of the calcium-activated potassium channels is large, these channels are almost always closed under physiological conditions (Findlay et al., 1985). Thus, doubt has been expressed that these channels can carry sufficient current to trigger the repolarization of the silent phase. Because ionic currents in the

0006-3495/89/08/229/14 $2.00

beta cell are small and delicately balanced, it is still possible to imagine that an average number of only one or two open Ca^{2+}-activated potassium per cell are sufficient to trigger bursting in coupled islet cells (Sherman et al., 1988).

Theoretical work by Chay has offered several other possible mechanisms for the triggering of bursting in the beta cell. Because the Ca^{2+}-activated potassium conductance is voltage-dependent, it has been proposed (Chay, 1986) that this channel, rather than the delayed rectifier, carries the outward current during the active phase. It has also been proposed that Ca^{2+}-inactivation of the inward calcium current (Chay, 1987), which has been observed experimentally in the beta cell (Plant, 1987), is responsible for the repolarization of the active phase, or that, perhaps, two calcium currents, one inactivated by calcium and the other not (Chay and Cook, 1988), are involved in bursting.

Another type of potassium channel, whose conductance is sensitive to ATP and ADP, has recently been documented in beta cells and other insulin secreting cell lines (Cook and Hales, 1984; Ashcroft et al., 1984; Misler et al., 1986; Rorsman and Trube, 1985; Ashcroft, 1987). These channels have a smaller unitary conductance but are more numerous ($\simeq$750/cell) than the Ca^{2+}-activated potassium channels. On the other hand, they are inactivated by ATP in detached patches, which is thought to explain their rapid inactivation by glucose in cell-attached patches. Recently, several groups have noted that ADP, when applied in physiological concentrations, can partially restore the activity of the ATP-sensitive potassium channel (Kakei et al., 1986; Dunne and Peterson, 1986; Ribalet and Ciani, 1986; Dunne et al., 1988). Because the activity of these channels is thus associated with glucose metabolism, it has been suggested that these channels may constitute a metabolic sensor for insulin release. Theoretical work using a glucose-inactivated potassium conductance further reinforces this idea (Rinzel et al., 1987).

Modulation of the activity of the ATP-sensitive channel by ADP has suggested another possible role for these channels in the beta cell (Misler et al., 1986; Keizer, 1988; Dunne et al., 1988). By responding to changes in the cytosolic ratio of ATP to ADP, the magnitude of their current may help control the duration of the active phase of bursting. For this suggestion to be plausible, cytosolic calcium, made available through the voltage-gated calcium channels would need to serve as a second messenger, decreasing the cytosolic ATP/ADP ratio. Because the concentrations of ATP and ADP are the order of millimolar in the beta cell (Kakei et al., 1986), the change in calcium concentration, which is the order of 0.2 μM, would need to be amplified some three to four orders of magnitude in order to modify the ATP/ADP ratio enough to affect the potassium conductance.

Here we investigate theoretically the possibility that calcium serves as a second messenger for activation and deactivation of the ATP/ADP modulated potassium channel during bursting (Keizer, 1988). In doing so we rely on experimental observations of the stimulating effect of ADP on the ATP-sensitive potassium channel (Kakei et al., 1986), the data of Rorsman and Trube (1986) to describe the voltage-gated calcium and potassium channels, and patch-clamp experiments on ATP-sensitive potassium channels to describe their current carrying properties (Misler et al., 1986; Rorsman and Trube, 1985). We examine several possible mechanisms by which cytosolic calcium could affect the cytosolic ATP/ADP ratio and conclude that the cycling of Ca^{2+} through the mitochondria via oxidative phosphorylation might provide sufficient amplification of the Ca^{2+} signal. We translate these ideas into a set of ordinary differential equations that describe the electrical activity of a islet cell. An analysis of these equations shows that they can support multiple steady states, action potential spikes, and, under appropriate conditions, bursting. The equations are solved numerically using physiologically reasonable parameters and the resulting electrical activity is found to be compatible with experiment, including glucose sensitivity. We embellish our calculations by adding the effect of Ca^{2+}-activated potassium channels. In the presence of both the ATP/ADP and Ca^{2+} modulated channels, we find reasonable bursting behavior, and conclude that a mixture of these two types of channels may be responsible for the triggering of bursting *in vivo*.

II. MODULATION OF ATP-SENSITIVE POTASSIUM CHANNEL

The conductance of the ATP-sensitive potassium channels in rat and mice beta cells has been found to depend on cytosolic ATP and ADP concentrations (Misler et al., 1986; Kakei et al., 1986; Dunne and Peterson, 1986; Ribalet and Ciani, 1987). ATP has a dual effect (Ohno-Shosaku et al., 1987). Initial challenges with micromolar to millimolar concentrations of ATP cause a substantial increase in closed time durations, thus decreasing the average conductance, without modifying unitary conductances. In the absence of MgATP, however, the channels experience "run down" of activity (Misler et al., 1986), a phenomenon that can be reversed by exposure to MgATP. The first effect is immediate and appears to be due to the binding of ATP to a regulatory site on the channel. The second phenomenon involves a longer time scale and may involve phosphorylation of the channel. As long as Mg^{2+}

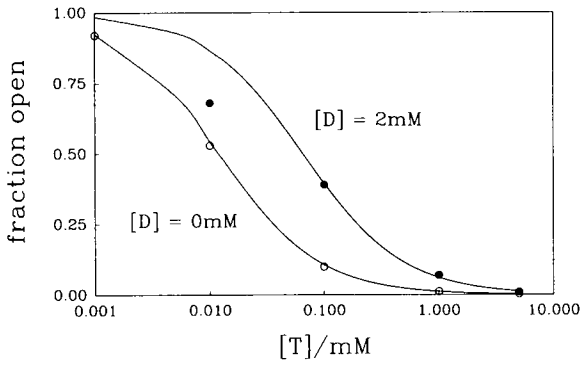

FIGURE 1 The solid lines represent fraction of open ATP-sensitive potassium channels as a function of the logarithm of the ATP concentration in millimolar as derived from Eq. 1 with K_1 = 0.45 mM and K_2 = 0.012 mM at ADP concentrations, [D], of 0 mM and 2 mM. The solid and open circles are measured data taken from Kakei et al. (1986).

ions are absent, the refreshment effect of ATP is not observed.

In the absence of ATP, millimolar concentrations of ADP also block the ATP-sensitive channel, while AMP has no discernible effect (Misler et al., 1986; Ribalet and Ciani, 1987). The action of ADP in the presence of ATP is quite different: ADP shifts the dose-response curve of current versus ATP concentrations to the right, thus desensitizing the channel to inhibition by ATP. This is illustrated in Fig. 1, where the data points are taken from Kakei et. al. (1986) and the smooth curves are drawn according to the formula:

$$i/i_0 = \frac{1 + [D]/K_1}{1 + [D]/K_1 + [T]/K_2}, \qquad (1)$$

where [D] and [T] are the concentrations of ADP and ATP, respectively, in millimolar units. Eq. 1 is appropriate for a mechanism involving competitive binding of ADP and ATP to the channel in which only the unbound state and the state with ADP bound are conducting. For a fixed concentration of ATP, Eq. 1 shows that the ATP/ADP ratio modulates the current through those channels such that a decrease in this ratio increases the current. For concentrations of ATP above 0.1 M, the fit with experiment is rather good, suggesting that competitive binding may be responsible for the desensitization of ATP by ADP.

In order for the desensitization of ATP by ADP to have an effect on electrical activity, it is necessary that one of the quantities involved in bursing modulate the ATP/ADP ratio. Indeed, the modulation must change the ADP concentration by the order of 0.1 mM or more because otherwise the effect on the dose response curve would be negligible (cf. Fig. 1). There is no evidence that the plasma membrane potential affects the ATP/ADP ratio and because the potassium concentration of the cells is effectively constant, one is left to consider the cytosolic calcium concentration. Although calcium affects the ATP/ADP ratio when pumped out of the cytosol by membrane bound calcium-ATPases, the net turn over of ATP is stoichiometric with calcium (McDaniel et al., 1985). Thus the action of these pumps can at most account for micromolar increases in ADP because at most micromolar changes in calcium occur in the cytosol during a burst of electrical activity. Indeed, to achieve the order of a 0.1 mM increase in ADP would require an effect of calcium on the primary mechanisms of ATP homeostasis in the cell.

In the beta cell both glycolysis and oxidative phosphorylation are involved in the production of ATP from glucose (Malaisse et al., 1983). Moreover, metabolites that are produced subsequent to glycolysis are known to mimic the stimulation of electrical activity by glucose. This suggests that if the modulation of the ATP/ADP ratio is involved in electrical activity, then the modulation probably occurs in the mitochondria.

There is other direct evidence that the mitochondria are involved in the control of electrical activity in the pancreatic beta cell. Indeed, the mitochondrial uncouplers carbonylcyamide trifluorpheylhydrazon (FCCP) and carbonylcyamide trichlorophenylhydrazone (CCCP), which short-circuit the proton motive force, have the effect of eliminating glucose-induced bursting by hyperpolarizing beta cells in whole islet preparations (Atwater et al., 1979). This has been interpreted as resulting from an increase in cytosolic calcium due to the elimination of calcium uptake by the mitochondria which, in turn, stimulates calcium-activated potassium channels in the plasma membrane. An alternative interpretation (Misler et al., 1986) is that disruption of the proton motive force by FCCP or CCCP, which decreases the ATP/ADP ratio by inhibiting oxidative phosphorylation, results in stimulation of ATP-sensitive potassium channels.

The mitochondria, in fact, are known to take-up and release calcium in the presence of the mitochondrial proton motive force (Carafoli and Crompton, 1977; Nicholls, 1982). The uptake and release occur through separate transporters, and at physiological calcium concentrations this leads predominately to a futile cycling of calcium. Because the futile cycling of calcium dissipates free energy that would normally be used in the synthesis of ATP, it seems plausible (Nicholls, 1982) that increases in cytosolic calcium, which increase the uptake rate, will slow the rate of ATP synthesis from ADP. Indeed, recent experiments in *Limulus* ventral photoreceptors (Fein and Tsacopoulos, 1988) have established that cytosolic cal-

cium stimulates rapid uptake of O_2 by mitochondria, which may be an indication of an uptake of calcium at the expense of ATP synthesis. Because the uptake of calcium and the synthesis of ATP both depend on the proton motive force, we are led to write the rate of mitochondrial synthesis of ATP in the canonical thermodynamic form (Keizer, 1987) as:

$$\text{Rate} = \Omega \exp\left(\frac{\Delta\mu_H + F\Delta\phi}{RT}\right) \exp(\mu_{ADP}/RT), \qquad (2)$$

where R and F are the gas and Faraday constants, T the absolute temperature, Ω is the intrinsic rate of synthesis, $\Delta\mu_H + F\Delta\phi$ is the proton motive force across the inner mitochondrial membrane, and μ_{ADP} is the chemical potential of the ADP in the matrix. Assuming that the proton motive force decreases with increasing calcium concentration, c, we expand the argument of the first exponential in a Taylor series and find that to first order the rate can be written as

$$\text{Rate} = \Omega \exp(r'[1 - c/r_1']) \exp(\mu_{ADP}/RT), \qquad (3)$$

where r' and r_1' are positive. Because r' is proportional to the proton motive force at low calcium, it will depend on the metabolic fuels creating the proton motive force. In particular, it should be an increasing function of glucose. The other parameter, r_1', determines the concentration range in which the effect of calcium on the mitochondria is appreciable, which we expect to be of the order of micromolar. Eq. 3 can be further simplified if we assume that the ADP in the matrix rapidly equilibrates with ADP in the cytosol so that $\mu_{ADP} = \mu_{ADP}^{cyt} \simeq \mu^0 + RT\ln[D]$. Thus defining $k' = \Omega \exp(\mu^0/RT)$, Eq. 3 can be written:

$$\text{Rate} = k' \exp(r'[1 - c/r_1'])[D]. \qquad (4)$$

In Appendix A we show how to use Eq. 4 to write the approximate rate of change of cytosolic ADP concentration as:

$$d[D]/dt = -k \exp(r[1 - c/r_1])[D] + k([A] - [D]), \qquad (5)$$

where $k' = k \exp(a)$, $r' = r + a$, and $r_1' = r_1 r'/r$. The second term takes into account the hydrolysis of ATP to ADP and P_i by reactions in the cytosol and $[A] \equiv [T] + [D]$ is treated as a constant. Eq. 5 is approximate for many reasons, including the neglect of glycolysis and the stimulation and/or inhibition of glycolysis by ATP, ADP, and AMP. Because it is impossible to characterize these phenomena without introducing a significant number of additional kinetic parameters, we restrict our characterization of ADP kinetics in the cytosol to Eq. 5. Note that the parameter $r = r' - a$ is an increasing function of glucose because r' is proportional to the proton motive force at low calcium concentration. Note also that the parameters r and r_1 determine to what extent the calcium signal will be amplified as it is transduced by the mitochondria into an ADP signal. According to Eq. 5, the rate of production of ATP from ADP decreases exponentially with the factor $\exp(-rc/r_1)$. Thus changes in the calcium concentration must be of the order r_1/r in order to have a significant effect on the ATP/ADP ratio.

III. MATHEMATICAL DESCRIPTION OF ELECTRICAL ACTIVITY

The effect of the ATP-sensitive channel on the behavior of the beta cell will be treated using an electrical circuit analogy like that employed in earlier descriptions of the beta cell (Chay and Keizer, 1983). This description appears to be appropriate for beta cells in intact islets or coupled together as clusters *in vitro* (Sherman et al., 1988). In this analogy the cell membrane is treated as a capacitive element with ion channels connected in parallel serving as resistors, each driven by the electromotive force resulting from the Nernst potential of the transported ion. Thus using Kirchoff's laws the transmembrane voltage, $V = \phi_{in} - \phi_{out}$, satisfies the equation

$$C dV/dt = -\sum_{k,j} g_{k,j}(V - V_k) = -\sum_{k,j} I_{k,j}, \qquad (6)$$

where C is the capacitance, $g_{k,j}$ is the conductance of the ions of kind k through channels of kind j and V_k is the Nernst potential

$$V_k = (RT/nF) \ln([k]_{out}/[k]_{in}), \qquad (7)$$

with n the charge of the ion. The conductances, $g_{k,j}$, are proportional to the total number of channels of kind j, which is assumed to be large so that the effect of single ion channel events can be neglected. Three types of conductances are used in our description: The voltage activated potassium and calcium ion conductances characterized by Rorsman and Trube (1986) and the ATP-sensitive potassium channel. As discussed in the preceding section, the activity of the ATP-sensitive channel is modulated by the ATP/ADP ratio according to Eq. 1. Thus because its conductance is voltage independent, we can write

$$I_{K,ATP} = \bar{g}_{K,ATP} \frac{(1 + [D]/K_1)(V - V_K)}{1 + [D]/K_1 + ([A] - [D])/K_2}, \qquad (8)$$

where $[A] \equiv [T] + [D]$. The value of $\bar{g}_{K,ATP}$ per cell can be estimated from the unitary conductance in physiological conditions (10–15 pS [Arkhammar et al., 1987]) and the number of channels (400–700 per cell [Rorsman and Trube, 1985]) to be in the range 4,000–10,000 pS. We chose a value of 7,500 pS. The values of K_1 and K_2 that fit the data of Kakei et al. (1986) in Fig. 1 are $K_1 = 0.45$ and $K_2 = 0.012$.

The voltage-activated potassium and calcium currents have been modeled in several different ways. We follow the lead of Sherman et al. (1988) who neglect the calcium inhibition of the calcium conductance, but add to their description the long-time scale (2.6 s) inhibition of the potassium channel (Rorsman and Trube, 1986) by introducing the time and voltage dependent inhibition, I. Thus we write

$$I_{K,V} = \bar{g}_{K,V} n I (V - V_K). \tag{9}$$

$$I_{Ca,V} = \bar{g}_{Ca,V} m_\infty(V) h(V) (V - V_{Ca}), \tag{10}$$

where n is the time and voltage-dependent activation for the potassium channel; $m_\infty(V)$ is the voltage-dependent activation of the calcium channel, taken as independent of time because of its rapid relaxation time (0.15–1.5 ms); and $h(V)$ is a voltage dependent factor to improve the fit of the current-voltage curves with experiment (Sherman et al., 1988). The time-dependent activation, n, and inactivation, I, satisfy the usual relaxation equations

$$dn/dt = -[n - n_\infty(V)]/\tau_n(V) \tag{11}$$

$$dI/dt = -[I - I_\infty(V)]/\tau. \tag{12}$$

Since Rorsman and Trube (1986) find τ to be 2.6 s and do not report its dependence on voltage, we have taken τ to be a constant. The mathematical expressions used to fit experimental measurements (Rorsman and Trube, 1986) for $m_\infty(V)$, $h(V)$, $n_\infty(V)$, $\tau_n(V)$, and $I_\infty(V)$ are given in Appendix B.

To complete the dynamical description, we use Eq. 5 to describe the rate of change to [D] and [T] = [A] − [D], the concentration of ADP and ATP, respectively, and introduce the usual balance equation (Chay and Keizer, 1983) to describe the change in cytosolic calcium, c:

$$f^{-1} dc/dt = -\alpha I_{Ca} - k_{Ca} c. \tag{13}$$

In this equation the factor $\alpha = 3{,}000/8\pi R^3 F$ with R the radius of a cell (in micrometers) converts current (in fA) to concentration per unit time (in micromole/millisecond); f is the fraction of calcium that is free in the cytosol; and k_{Ca} is the first order rate constant for extrusion of calcium from the cytosol.

Eqs. 5–13 differ in several ways from previous differential equations used to describe the beta cell. First, the calcium concentration does not have a direct feed back onto a potassium current, but, instead, effects the ATP/ADP ratio through Eq. 5, which in turn modulates the current in the ATP-sensitive potassium channel. Thus instead of a single variable, there are two variables in the feed back link, c and [D]. Calcium, as Rinzel (1985) has pointed out, is a "slow" variable whose characteristic time scale is set by the parameter, f, to be the order of a second. The parameter k in Eq. 5 sets the time scale for the concentration of ADP. When $k < 10^{-3}$ ms^{-1} then [D] is also a slow variable, whereas when $k > 1$ ms^{-1} it varies on a characteristic time scale of milliseconds and so is a "fast" variable. Because it is coupled directly only to the slow variable, c, if [D] is fast, then it rapidly adjusts its value so that the left hand side of Eq. 5 vanishes, giving

$$[D] = \frac{[A]}{1 + \exp\,[r(1 - c/r_1)]}. \tag{14}$$

Accordingly, when k is large [D] is so tightly coupled to c that its instantaneous value is determined by the functional relationship in Eq. 14. Note that in this situation [D] is an increasing function of c. Thus as c increases, the ATP/ADP ratio decreases, leading via Eq. 8 to an activation of the current carried by the ATP-sensitive potassium channel. Indeed, for the values of $r_1 = 0.5$ μM and $r \simeq 1$ used in the calculations that follow, [D] and c are approximately linearly related in the physiological regime of concentrations with a slope $d[D]/dc \simeq 3$ mM/μM. This provides the amplification of the calcium signal from the micromolar concentration range to the millimolar range of ADP.

The original proposal for calcium feed back on electrical activity involved direct activation of a potassium conductance by calcium (Atwater et al., 1980; Chay and Keizer, 1983). Following Plant (1978), that has been modeled by the following simplified current expression

$$I_{K,Ca} = \bar{g}_{K,Ca} \frac{(c/K_D)(V - V_K)}{1 + c/K_D}. \tag{15}$$

While there is evidence that this current is voltage-dependent (Findlay et al., 1985), present data suggests that this effect is small in the physiological regime. It seems likely that both the ATP-sensitive and calcium-activated potassium channels carry current during bursting, and we examine their combined effect in Section V.

IV. ANALYSIS OF DYNAMICAL EQUATIONS

The dynamical equations that describe the membrane potential of the beta cell in this model are given in Eqs. 7–13, 1-B, and 2-B. Following Rinzel (1985) we analyze their behavior in terms of fast and slow subsystems of equations. To simplify this analysis somewhat we assume that the parameter k is sufficiently large ($k > 1$ ms^{-1}) that Eq. 14 is valid. This leaves two variables in the fast subsystem, n and V. Their characteristic time constants are the order of 20–40 ms, as can be estimated from Eqs. 8–10, B-1, and B-2 using the parameters and "typical" values of the variables given in Table 1. The slow variables are [c] and I. However, under the assumption

TABLE 1 Standard parameter values and typical values of variables*

Parameters‡		
A	Total ATP + ADP	5 mM
$\bar{g}_{K,ATP}$	Maximal conductance per cell, ATP sensitive K^+ channels	7,500 pS
K_1	ADP binding constant, ATP-sensitive K^+ channels	0.45 mM
K_2	ATP binding constant, ATP-sensitive K^+ channels	0.012 mM
$\bar{g}_{K,V}$	Maximal conductance per cell, voltage-gated K^+ channels	2,500 pS
$\bar{g}_{Ca,V}$	Maximal conductance per cell, voltage-gated Ca^{2+} channels	1,400 pS
$\bar{g}_{K,Ca}$	Maximal conductance per cell, Ca^{2+}-activated K^+ channels	35,000 pS
K_D	Ca^{2+} binding constant, Ca^{2+}-activated channels	100 μM
λ	Dimensionless time constant parameter for voltage-gated K^+ channels	1.5
C	Capacitance of beta cell	5310 fF
R	Radius of beta cell	6.5 μm
f	Fraction of Ca^{2+} that is free	0.001
r	Glucose-sensitive mitochondrial rate parameter	1.5
r_1	Calcium-sensitivity of mitochondrial proton-motive force	0.5 μM
k	Rate constant for ATP hydrolysis	10 ms^{-1}
τ	Time constant for inactivation, I	2.6 s
V_K	Nernst potential for K^+	−75 mV
V_{Ca}	Nernst potential for Ca^{2+}	110 mV
k_{Ca}	Rate constant for Ca^{2+} uptake	0.06 ms^{-1}
Variables		
V	Membrane potential	−60 mV to −20 mV
c	Cytosolic free calcium concentration	0.1 μM to 0.4 μM
[D]	Cytosolic ADP concentration	2.0 mM to 2.1 mM
n	Activation of g_K	0.0002 to 0.16
I	Inactivation of g_K	0.85 to 0.95

*See Sherman et al. (1988), Rorsman and Trube (1986), and the discussion in Section III.
‡Values of other channel parameters given in Appendix B.

that k is large, [D] takes the place of c as a slow variable. Indeed, Eqs. 13 and 14 imply that

$$d[D]/dt = \frac{[A](r/r_1)\exp[r(1 - c/r_1)]f}{\{1 + \exp[r(1 - c/r_1)]\}^2}(-\alpha I_{Ca} - k_{Ca}c), \quad (16)$$

where c is the function of [D] obtained by inverting Eq. 14. Because the factors (r/r') and exponentials are near unity, it follows that f determines the time scale for the relaxation of [D], which is the order of seconds. Thus [D] now appears as a slow variable with a relaxation time comparable to I, namely, $\tau = 2.6$ s. Because the characteristic relaxation times for the fast (n and V) and slow ([D] and I) variables are separated by nearly two orders of magnitude, the dynamical states of the entire system of equations can be analyzed by treating the slow variables, [D] and I, as fixed parameters in the first subsystem, V and n. Once the parametric behavior of the fast system is known, superimposing the slow dynamics of [D] and I generally provides a simple understanding of the behavior of the complete system.

The primary advantage of the separation into fast and slow variables is that it allows one to analyze a complex dynamical problem using its fast and slow components, each of which is generally simpler to understand. For example, for the Chay-Keizer model (Rinzel, 1985) the fast-slow analysis explicitly shows that the dynamics of the active phase are dominated by potassium-calcium action potential spikes, while the magnitude of the bursting period is dominated by calcium handling mechanisms. The fast-slow separation is particularly useful for the present mechanism, which is complicated by the presence of two fast and two slow variables.

The dynamical behavior of the complete system of equations, integrated using the PLOD implementation (Kahaner and Barnett, 1988) of the Gear algorithm (Hindmarsh, 1974), is shown in Fig. 2 for three sets of values of the glucose dependent parameter r. As this parameter is increased, corresponding to an increase in the concentration of glucose, there is a change in the pattern of voltage oscillations from bursting with a long silent phase ($r = 1.0$), to bursting with a short silent phase ($r = 1.5$), to continuous spiking ($r = 2.0$). For smaller values of r (low glucose) the voltage is polarized to a constant value of ~ -65 mV, while for significantly larger values of r one finds continuous spiking of higher frequencies. In Fig. 2 we have also plotted the calcium and ADP concentrations during bursting and spiking. As r is increased the average concentration of ADP stays in the range of 2.05 to 2.08 mM while the average calcium concentration increased by $\sim 1/3$. We note, also, that the frequency of the action potential spikes decreases towards the end of a burst, as found both experimentally and in other models of beta cell electrical activity. From the data in these figures we can estimate using Eq. 1 that only 1–2% of the ATP-sensitive channels are open during bursting, which is compatible with data from patch clamp experiments showing that glucose greatly reduces the fraction of open channels in cell attached patches (Arkhammer et al., 1987; Ribalet and Ciani, 1987). While the calculations in Fig. 2 were carried out with the parameter $k = 10$ ms^{-1}, only minor differences were found when k was decreased by up to four orders of magnitude.

The application of Rinzel's slow and fast variable analysis to understand this dynamical behavior is straight

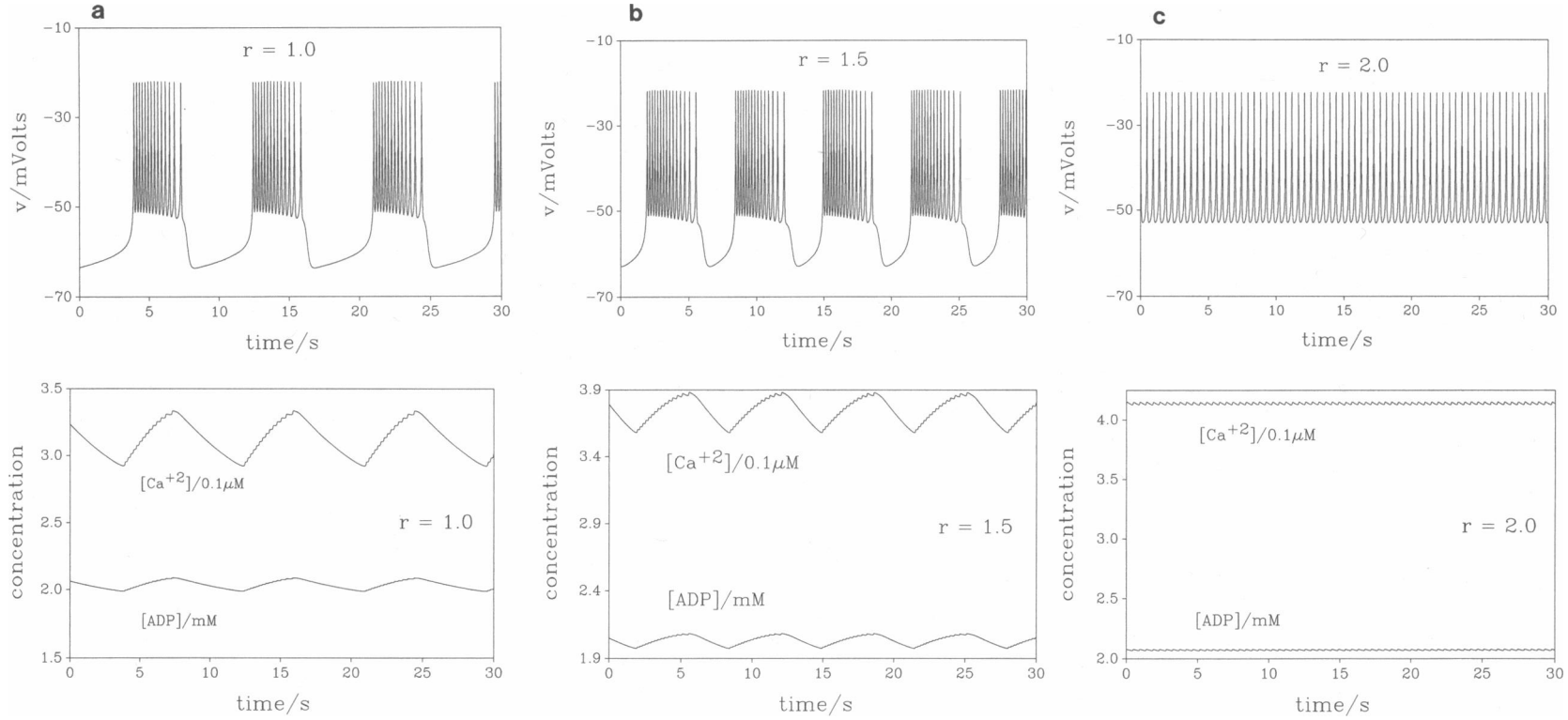

FIGURE 2 (*a*) The calculated voltage, calcium, and ADP oscillations as a function of time for the glucose-dependent parameter $r = 1.0$. Other parameters are as described in the text. (*b*) As in Fig 2 *a*, except $r = 1.5$. (*c*) As in Fig. 2 *a*, except $r = 2.0$

forward (Rinzel, 1985; Rinzel and Lee, 1987). To do so we first treat the slow variables I and [D] as constants and determine the steady state voltage as a function of [D] with I as a parameter. This is accomplished by setting the left hand sides of Eqs. 6 and 11 equal to zero, which leads to the typical z-shaped curves shown in Fig. 3 *a* for I = 0.00, 0.50, and 1.00. The stability of these states can be tested using the dynamical equations for the fast variables (V and n) with I and [D] fixed. We have used both direct integration of the equations of motion (the Gear algorithm) and the automated bifurcation program, AUTO (Doedel, 1981), for this purpose. One finds that the steady states on the central branch (between the two knees of the z-curve) are unstable (*dashed lines*) for all values of I, while the low voltage branch of steady states (to the right of the lower knee) are stable (*full line*). For states on the upper branch the situation is more complicated. For example, when $I \geq 0.30$ some of the states, those lying to the right of a Hopf bifurcation point (*open circle*), are unstable. To the left of the Hopf bifurcation oscillations are damped and the steady states are stable, while to the right of the Hopf point the damping disappears and stable oscillations in n and V occur. For $I \geq 0.30$ there is another interesting point to the right of the Hopf point called a homoclinic point. This point is defined by the intersection of the V-n limit cycle (for fixed [D] and I) with the central branch of unstable status. For I = 0.50 and 1.00 the homoclinic points are indicated in Fig. 3 *a* by closed circles. As [D] approaches the homoclinic point from below, the period of the oscillations grows to infinity.

If I is increased well above 0.30, the Hopf point moves to the left to smaller values of [D] and the homoclinic point moves down along the central branch of the z-curve. For example, at I = 0.50, $[D]_{Hopf}$ = 1.97 and $[D]_{homo}$ = 2.21, while at I = 1.00 $[D]_{Hopf}$ is negative and $[D]_{homo}$ is 2.09. For $I \geq 0.30$ the maximum amplitude of the limit cycle spikes depends on the value of [D], increasing from zero at the Hopf points to values near the homoclinic points of 24 mV for I = 0.50 and 29 mV for I = 1.00.

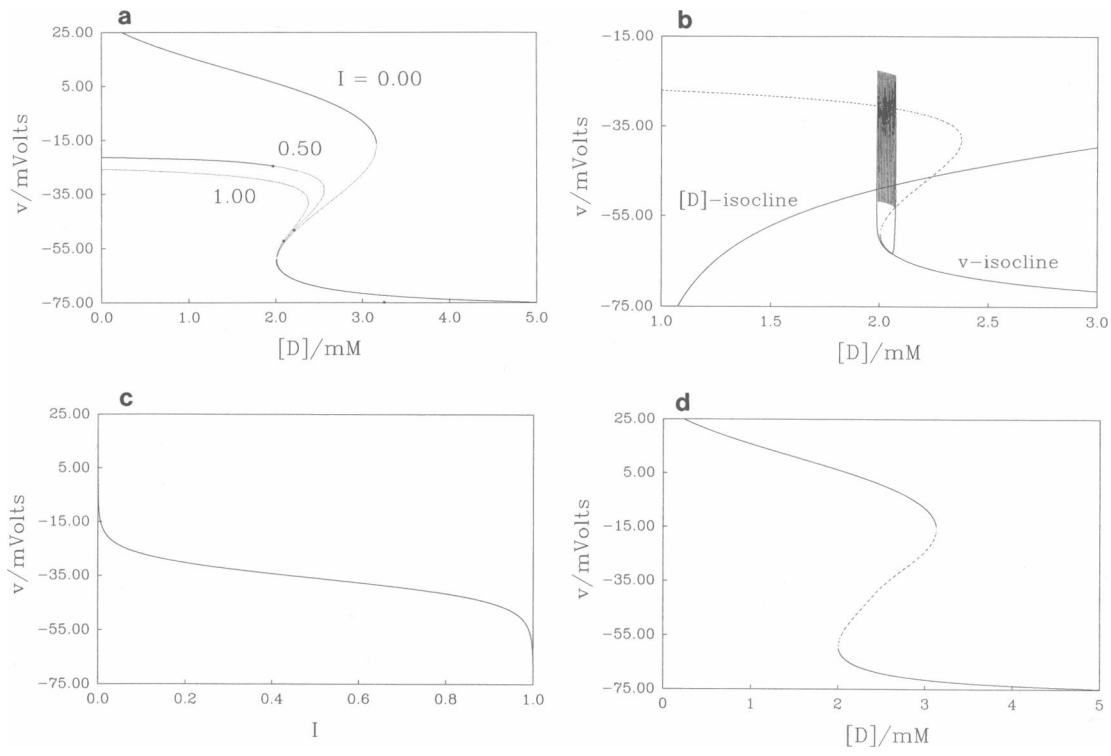

FIGURE 3 (*a*) The z-curves for I = 0.00, 0.50, and 1.00 obtained by setting the right-hand-side of Eqs. 6 and 11 equal to zero and solving for V as a function of [D], i.e., the intersections of the V- and n-isoclines for various fixed values of I with other parameters as described in the text. The dashed lines represent unstable steady states at fixed [D], while the full lines are stable. The open circle is the Hopf point for I = 0.50 and the filled circles are homoclinic points for I = 0.50 and I = 1.00. (b) The [D]-isocline obtained by setting the right-hand-side of Eq. 5 equal to zero. Superimposed on this is the z-curve for I = 1.00, which intersects the [D]-isocline at an unstable steady state. The burst trajectory for r = 1 has also been included in the figure. (*c*) The I-isocline obtained by setting the right-hand-side of Eq. 12 equal to zero. (*d*) The z-shaped curve obtained by setting the right-hand-side of Eqs. 6, 11, and 12 equal to zero, i.e., the intersection of the V-, n-, and I-isoclines projected into the V-[D] plane.

This behavior of the fast system of V and n allows one to understand why bursting appears in this model. The reason is simple, essentially that found by Rinzel (1985), except in the present case there are two slow variables, I and [D]. Consider, first, the case that I is fixed and large enough ($I \geq 0.30$) so that the Hopf point on the upper branch is to the left of both the lower knee and the homoclinic point, which is to the right of the lower knee (cf. Fig. 3 *a*). The curve on which $d[D]/dt$ vanishes (the [D]-isocline), which according to Eq. 16 is independent of I, is shown in Fig. 3 *b* for the standard parameter values in Table 1. The intersection of this curve with the z-curve for fixed I determines the steady state, which as illustrated in Fig. 3 *b* for $I = 1.00$, is on the unstable branch of the fast system. Thus there is no stable steady state, and the time dependence of the system V, n, [D] with I fixed can be understood by taking [D] as a slow time-dependent parameter for the fast system.

To see how this works, assume for definiteness that the values of V and [D] lie on the lower branch of steady states. Because Fig. 3 *b* shows that there [D] is to the right of its isocline, it follows that [D] decreases while V remains on the lower branch of the z-curve. When V and [D] move just beyond the lower knee, V is attracted rapidly to the limit cycle on the upper branch. The limit cycle on the upper branch, however, is to the left of the [D]-isocline, so that [D] now increases. As a consequence, the trajectory is swept through the manifold of limit cycles for the fast system (V, n) in the direction of the homoclinic point. When [D] passes the homoclinic point, the only remaining attractor for the fast system is on the lower branch of the z-curve, and V rapidly decreases, completing the bursting cycle. This trajectory is illustrated in Fig. 3 *b*. Thus bursting, for fixed I, can be understood in terms of the slow variable [D] periodically sweeping upwards through the limit cycle spikes on the upper branch and then downwards through the stable steady states on the lower branch.

The dynamical behavior with I free to vary according to Eq. 12 can be understood in a comparable fashion. The isocline for I, which is found from Eq. 12 to be $I = I_\infty(V)$, is independent of [D]. Its functional form is plotted in Fig. 3 *c* for the standard parameter values in Table 1. To visualize the dynamical effect of I, it is convenient to imagine an I-axis perpendicular to the plane of the z-curves in Fig. 3 *a* and extending into the page. In this three-dimensional space of I, [D], and V the z-curves become a z-surface extending into the page with a lower branch that has no outward tilt in the positive I-direction. The upper branch, on the other hand, is tilted with the curve defining the locus of the upper knees angled to the left. Because the surface of [D]-isoclines is independent of I, by comparing Figs. 3 *a* and *b* it is easy to visualize that the line of its intersections with the two-dimensional z-surface remains on the unstable center branch of the z-curves.

To help with this visualization the projection into the V-[D] and I-[D] planes of the intersection of several important curves with the z-surface are shown in Fig. 4. Because the I-isocline in Fig. 3 *c* is a surface independent of [D], it is also easy to see that it intersects the z-surface in a line that lies on the upper branch (near $I = 0$), on the lower branch (near $I = 1$), and on the central (unstable) branch. The projection of this line onto the I-[D] plane is given in Fig. 4 *b*. Because for the standard parameter values the surface of [D]-isoclines intersects only the central branch, the complete system has a unique steady state that is unstable.

Bursting in the complete system (I, V, n, and [D]), as shown in Fig. 2, is a limit cycle that circles near this

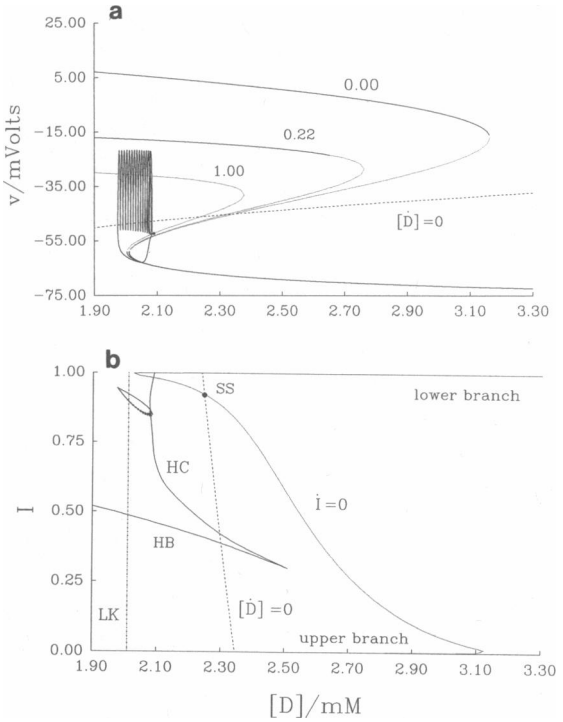

FIGURE 4 (*a*) The z-curves for $I = 0.00$, 0.22, and 1.00 shown together with the projection of the [D]-isoclinal surface ($[\dot{D}] = 0$) and the projection of the time course of one burst for $r = 1.5$ into the V-[D] plane. (*b*) The projection into the I-[D] plane of the intersection of the [D]-isoclinal surface with the z-surface (*dashed line*) and the intersection of the I-isoclinal surface with the z-surface (*dotted line*) shown on the same [D]-scale as Fig. 4 *a*. Also shown are the projections into this plane of the Hopf points (HB) and homoclinic points (HC) for the fast subsystem, the lower knee (LK) of the z-surface, and the time course of one burst for $r = 1.5$ (*closed curve* in upper left corner). Note that the I-isoclinal surface intersects the upper branch of the z-surface near $I = 0$ and the lower branch near $I = 1$. Below $I = 0.30$ the value of [D] at the Hopf point is smaller than the value of [D] at the homoclinic point and, thus, the limit cycle for the fast system is unstable.

unstable state with $I \geq 0.85$. The projection of this trajectory onto the I-[D] plane, along with the projection of the homoclinic points (HC) when [D] and I are held constant, are shown in Fig. 4 *b*. Note that the trajectory moves from the active to the silent phase at a homoclinic point, as predicted by the fast-slow analysis, but overshoots considerably the lower knee (LK) before returning to the active phase. The lower branch of the z-surface, in this range of values for I, is below the I-isoclinical surface, in this range of values for I, is below the I-isoclinal surface. Thus on a trajectory in this region I increases until [D] and V get beyond the lower knee of the z-surface (Fig. 4 *a*). This forces V to increase rapidly to the upper branch, thence, bringing I above its isocline. This causes I to decrease on the slow time scale until [D] and V reach the homoclinic point, where the trajectory then returns rapidly to the lower branch. Because the isoclinal surface for I intersects the upper branch only near $I = 0$, the slow time scale for the change of I guarantees that this part of phase space will not be visited during a burst. On the other hand if τ, the relaxation time for I, is reduced from 2.6 s to 50 ms (so that I is also a fast variable), the spiking electrical activity characteristic of bursting disappears. It is replaced by a limit cycle that oscillates between the lower branch of the z-surface near $I = 1$ and the upper branch near $I = 0$ (cf. Fig. 4 *b*), with only vestigial spikes remaining as the voltage switches from the lower to the upper branches.

It is not hard to see that the slow variable [D] is an essential slow variable contributing to bursting, but that I is not. This can be done by treating [D] as a constant parameter and examining the dynamics of V, n, and I. Because I solves Eq. 12, which depends only on V, the projection of the intersection of the V-isocline with the n- and I-isoclines onto the V-[D] plane can be obtained by setting $dV/dt = 0$ in Eq. 6, $dn/dt = 0$ in Eq. 11, and substituting $I_\infty(V)$ for I in Eq. 9. The resulting curve provides the steady state values of V as a function of [D] and is given in Fig. 3 *d*. This curve has a z-shape and closely resembles the $I = 0$ curve in Fig. 3 *a*. For [D] smaller than the left knee or larger than the right knee there are stable states on the upper branch (near $I = 0$) and lower branch (near $I = 1$), respectively, while for each [D] between the knees there are steady states. When the differential equations are solved for V, n, and I with [D] fixed, we find only trajectories that relax to the upper and lower branch of steady states. Thus unless [D] is allowed to vary there are no limit cycles and no bursting. Further evidence that I is not an essential slow variable can be obtained by changing its characteristic time parameter, τ. We find that with [D] fixed the intrinsic stability of the upper and lower branches is unaffected by alterations in τ. Thus no matter how slow or fast the variable I is, unless [D] can change only transient electrical activity is found.

Throughout the analysis in this section we have assumed that the coupling parameter k in Eq. 5 was large enough that ADP and calcium were tightly coupled, as in Eq. 14. This reduced the number of variables to four and the number of slow variables to two. While a complete analysis of the effects of varying k will not be attempted here, the limit that k approaches zero, which makes [D] a third, and the slowest, slow variable, is easy to understand. Indeed, in the limit that $k = 0$, [D] becomes a constant. This is precisely the situation examined in the previous paragraph, which implies that only steady states will be observed. If k is not precisely zero (say, $k = 10^{-5}$), then the slow change in [D] can lead to a limit cycle in which most of the time is spent at a hyperpolarized and at a depolarized quasi-steady state with periodic excursions between the two, the depolarizing excursion involving transient spiking. The behavior for somewhat larger values of k is more complex and will be described elsewhere (Magnus, G., manuscript in preparation).

V. GLUCOSE DOSE-RESPONSE

The electrical activity of the beta cell responds in a sensitive fashion to changing concentrations of glucose and other of its metabolites. In Section III we proposed that the mitochondria provide this sensitivity through the chemiosmotic gradient, which affects the ATP/ADP ratio in the cytoplasm. The impact of this on electrical activity is determined through the dependence of the ATP-sensitive potassium channels on this ratio. In this picture the effect of glucose is an indirect one and would be mimicked by other metabolites that either feed into the citric acid cycle or otherwise stimulate oxidative phosphorylation.

The most important physiological consequence of glucose stimulation is insulin secretion, which has been shown to be correlated with glucose-stimulated electrical activity (Meissner, 1976). While the detailed mechanism connecting these two phenomena is as yet unknown, it is widely assumed that increases in cytosolic calcium associated with spiking provide a link between electrical activity and secretion. Thus one measure of the glucose dose-response for the beta cell is the cytosolic calcium concentration as a function of the stimulatory concentration of glucose (Himmel and Chay, 1987; Rinzel et al., 1987). As we have already seen, in our model the parameter r increases with the proton motive force and, thus, it is an increasing function of glucose. The general effect of r on the time course of cytosolic calcium is shown in Fig. 2 during bursting ($r = 1.0$ and 1.5) and spiking ($r = 2.0$).

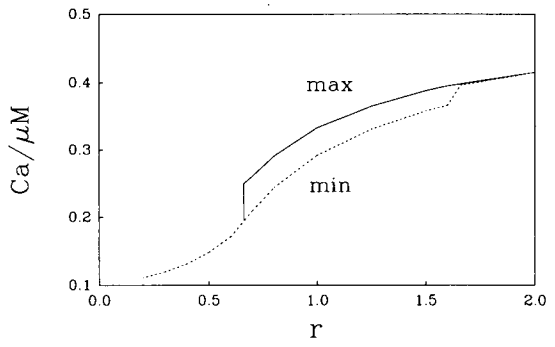

FIGURE 5 The calculated cytosolic calcium concentration as a function of the glucose-dependent parameter, r. "max" refers to the maximum calcium value and "min" to the minimum value during oscillations. There is an abrupt increase in the response just below the threshold to bursting at $r_B = 0.66$ and a leveling off near the threshold to continuous spiking at $r_{CS} = 1.64$.

The average calcium concentration obviously increases as r increases.

This effect is investigated more completely in Fig. 5, where maximum and minimum calcium concentrations are shown as a function of r for the standard parameter values. Below $r_B = 0.66$, there is a single stable steady state with a calcium concentration of ~0.1 μM. This corresponds to low ambient glucose concentrations and an absence of electrical activity. Between $r_B = 0.66$ and $r_{CS} = 1.64$ bursting is observed, with maximum and minimum calcium concentrations increasing as r increases in this range. Above $r_{CS} = 1.64$ one has continuous spiking, which is chaotic below $r = 1.70$. While the value of the calcium concentration is not fixed during continuous spiking, its maximum and minimum are nearly indistinguishable on the scale of the graph, and their values increase relatively slowly with r. The overall behavior in Fig. 5 is qualitatively similar to that found in Himmel and Chay (1987) and Rinzel et al (1987), who used the Chay-Keizer minimal model with a constant glucose-dependent conductance representing the effect of the ATP-sensitive channels. Notice that the average calcium concentration changes by a factor of two from the onset of bursting at r_B to the onset of continuous at r_{CS}. While the magnitude of this increase depends on the other parameters used in the calculation, glucose-induced increases in cytosolic calcium in just this range of concentrations recently have been observed in isolated beta cells (Rorsman et al, 1984; Arkhammer et al, 1987).

The dose-response curve for glucose induction of electrical activity can be modified by increasing the external calcium concentration or by adding sulphonylureas to the external medium (Atwater, 1988). In sufficient concentrations sulphonylureas are known to completely inhibit the ATP-sensitive potassium channel (Trube et al., 1986) in what is thought to be a selective fashion, and these compounds are well known to produce continuous spiking in bursting islet cells (Meissner and Atwater, 1976). The fact that bursting can be restored at a fixed glucose concentration by increasing the calcium concentration in the external medium (I. Atwater, personal communication) suggests that additional channels may be involved in the control of bursting. While we defer a more complete treatment of this subject, in light of the above experiments it seems important to show that the electrical behavior found in our calculations is not changed dramatically if additional types of potassium channels are present.

For simplicity, we do this using the Ca^{2+}-activated potassium current given in Eq. 15. The only modification that this makes in our differential equations is to add this current to the three existing currents Eqs. 8–10 on the right side of the differential equation for the voltage, Eq. 6. Using the values of K_D and $\bar{g}_{K,Ca}$ given in Table 1 along

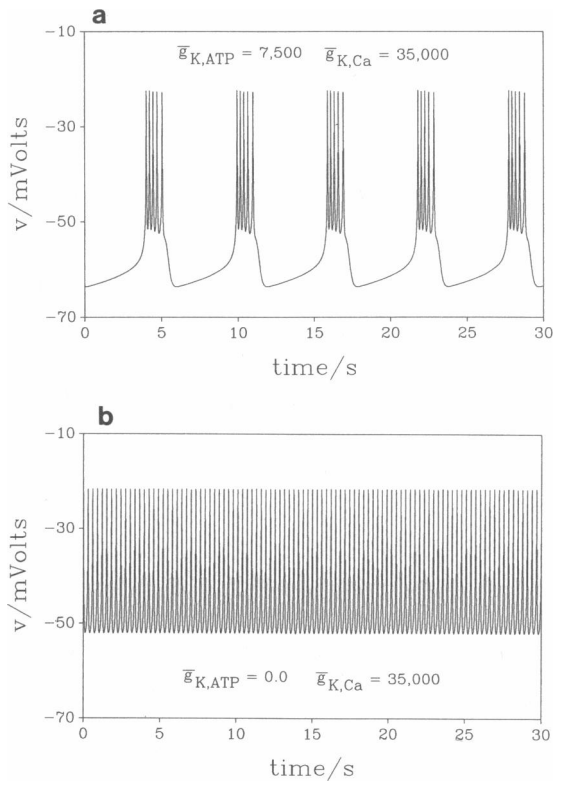

FIGURE 6 (*a*) Modification of the calculated bursting pattern in Fig. 2 *b* with a mixed population of ATP-sensitive and calcium-activated potassium channels. Maximal conductances per cell are $\bar{g}_{K,ATP} = 5{,}000$ and $\bar{g}_{K,Ca} = 35{,}000$, with other parameters as in Table 1 and in Appendix B. (*b*) The continuous spiking that results for the system in Fig. 6 *a* when the parameter $\bar{g}_{K,ATP}$ is set equal to zero.

the $\bar{g}_{K,ATP}$ = 5,000 and the other standard parameter values, the resulting solution for the voltage is given in Fig. 6. Comparing with Fig. 2 for r = 1.5, the primary effect of the Ca^{2+}-activated potassium channel is seen to be a shortening of the active phase and a lengthening of the silent phase. Otherwise all of the qualitative features of the electrical activity remain unaltered. Using these same conductances the effect of glyburide in inhibiting the ATP-sensitive channel can be examined by setting $\bar{g}_{K,ATP} = 0$. This leads to the continuous spiking shown in Fig. 6, in agreement with experiment. On the other hand, in the absence of the Ca^{2+}-activated potassium channels, the effect of setting $\bar{g}_{K,ATP} = 0$ is to depolarize the membrane to the calcium reversal potential of +110 mV, because the inhibition factor, I, greatly reduces the voltage-activated potassium current at positive voltages. This reinforces the notion that the full range of electrical activity of the beta cell involves more than just the ATP-sensitive channel. The consequences of this conclusion will be explored more fully in future publications.

VI. SUMMARY AND CONCLUSIONS

Our purpose has been to make plausible the notion that the ATP-sensitive potassium channel possesses sufficient regulatory properties to serve as the control channel for electrical bursting in the pancreatic beta cell. In doing so we have relied on the experimental fact that ADP shifts the ATP inactivation curve to the right, thereby increasing the conductance of the ATP-sensitive channels (Kakei et al., 1986). In this way modulation of the ATP/ADP ratio serves to increase the activity of these channels. Because the ATP/ADP ratio depends on the metabolic state of the cell, this provides a direct mechanism for glucose sensing.

In order for this mechanism to lead to bursting, it is necessary that the voltage-gated channels in the beta cell affect the ATP/ADP ratio in some fashion. The way that we have imagined this happening is through the proton motive force of the mitochondria, which is reduced by calcium ions brought into the cytoplasm by voltage-gated calcium channels. The reduction of the proton motive force tends to decrease the ATP/ADP ratio and, thereby, activate the ATP-sensitive conductance.

When these qualitative notions are expressed as a quantitative mathematical model, we find that the solutions to the resulting differential equations exhibit electrical activity similar to that observed experimentally. This includes a hyperpolarized state at −65 mV at parameter values corresponding to low glucose concentrations; bursting at intermediate glucose concentrations; and continuous spiking at high glucose concentrations. The calculations show that cytosolic calcium concentration increases from a value near 0.1 μM at low glucose to a value near 0.4 μM at high glucose concentrations, in agreement with measurements on isolated beta cells. Although in the calculations presented here we have assumed that ADP and cytosolic calcium are tightly coupled dynamically as in Eq. 14, this is not necessary and comparable results are found even when the coupling constant k is reduced by four orders of magnitude to 0.001 ms^{-1}.

The mathematical features of the model are somewhat more complicated than previous models of the beta cell, because it involves two intrinsically slow variables, namely, ADP and the inactivation, I. Following the lead of Rinzel (1985), we show that bursting can be understood in terms of the dynamical behavior of two fast variables (the voltage, V, and activation, n) on which is superimposed slow changes in the two parameters representing the slow variables. For this model, the concentration of ADP is the crucial slow variable, which serves as the trigger that causes transitions between the active and silent phases.

The analysis here relies heavily on the regulatory properties of the ATP-sensitive potassium channel. Indeed, it is this channel exclusively that responds to the trigger variable, ADP. Nonetheless, it seems likely that other potassium channels, e.g., Ca^{2+}-activated channels, may share in the regulation of the electrical activity. Adding a simplified version of the conductance of these channels to our model, we find only small quantitative changes in the results of our calculations. Based on our results it seems likely that a proper mix of regulated potassium channels is necessary to explain pharmacological modifications of the glucose dose-response curves and other experiments on intact islets. Whether the ATP-sensitive channel will occupy a major role in explaining these more complex experiments remains to be seen.

APPENDIX A

Assuming that ADP also rapidly equilibrates between the mitochondrial matrix and the cytosol, the time rate of change of cytosolic ADP is given by the sum of its rate of loss in the mitochondria and its rate of change in the cytosol. The primary processes creating cytosolic ADP are enzyme catalyzed hydrolysis of ATP and the conversion of ATP and AMP to 2 ADP catalyzed by adenylate kinase, whose rates can be written

$$(d[D]/dt)_{cyt} = k[T], \quad \text{(A-1)}$$

where k is a pseudo-first order rate constant and [T] is the concentration of ATP. Because oxidative phosphorylation seems to be the primary source of ATP during respiration, we neglect the effect of glycolysis. Thus combining Eqs. 4 and A-1 gives

$$d[D]/dt = -k \exp[r(1 - c/r_1)][D] + k([A] - [D]), \quad \text{(A-2)}$$

where $[D] + [T] = [A]$, $k' = k \exp(a)$, $r = r' - a$, and $r_1 = r_1' r/r'$.

APPENDIX B

The forms of the functions $m_\infty(V)$, and $I_\infty(V)$ used to describe the voltage activated potassium and calcium conductances in Eqs. 9 and 10 are

$$j_\infty(V) = 1/\{1 + \exp[(V_j - V)/S_j]\}, \qquad \text{(B-1)}$$

where $j = m$, n, or I. Specific values are $V_m = 4$ mV, $V_n = -15$ mV, $V_I = -36$ mV and $S_m = 14$ mV, $S_n = 5.6$ mV, $S_I = -4.1$ mV. The function $h(V)$ is fit by a similar functional form with $V_h = -10$ and $S_h = -10$. The relaxation time, $\tau_n(v)$, in milliseconds is taken as

$$\tau_n(V) = \frac{60/\lambda}{\exp[(V + 75)/65] + \exp[-(V + 75)/20]} \qquad \text{(B-2)}$$

with V, as usual, in millivolts, and $\lambda = 1.5$.

This work originated while J.K. was a John Simon Guggenheim Fellow at the National Institutes of Health and benefited greatly from conversations with and comments from Drs. J. Rinzel, I. Atwater, A. Sherman, and S. Misler. We also thank Prof. G. R. Welch for providing computer time at the University of New Orleans.

Support for this work came from National Science Foundation grant CHE 86-18647 and the Agricultural Experiment Station of the University of California, Davis.

Received for publication 7 November 1988 and in final form 3 March 1989.

REFERENCES

Arkhammar, P., T. Nilsson, P. Rorsman, and P. -O. Berggen. 1987. Inhibition of ATP-regulated K^+ channels precedes depolarization-induced increase in cytoplasmic free Ca^{2+} concentration in pancreatic beta cells. *J. Biol. Chem.* 262:5448–5453.

Ashcroft, F. M. 1988. Adenosine 5'-triphosphate-sensitive potassium channels. *Annu. Rev. Neurosci.* 11:97–135.

Ashcroft, F. M., D. E. Harrison, and S. J. H. Ashcroft. 1984. Glucose induces closure of single potassium channels in isolated rat pancreatic β-cells. *Nature (Lond.).* 312:446–448.

Atwater, I., C. M. Dawson, B. Ribalet, and E. Rojas. 1979. Potassium permeability activated by intracellular calcium ion concentration in the pancreatic beta cell. *J. Physiol. (Lond.).* 288:575–588.

Atwater, I., C. M. Dawson, A. Scott, G. Eddlestone, and E. Rojas. 1980. The nature of the oscillatory behavior in electrical activity for pancreatic β-cell. *J. Horm. Metabolic Res.* 10:(Suppl.)100–107.

Atwater, I., E. Rojas, and B. Soria. 1987. Biophysics of the Pancreatic Beta Cell. Plenum Publishing Corp., New York.

Carafoli, E., and M. Crompton. 1977. *Curr. Topics Membr. Transp.* 10:151–216.

Chay, T. 1986. On the effect of intracellular calcium-sensitive potassium channels in the bursting pancreatic beta cell. *Biophys. J.* 50:756–777.

Chay, T. 1987. The effect of inactivation of calcium channels by intracellular calcium ions in the bursting pancreatic beta cells. *Cell Biophys.* 11:77–90.

Chay, T., and D. Cook. 1988. Endogenous bursting patterns in excitable cells. *Math. Biosci.* 90:139–153.

Chay, T. R., and J. Keizer. 1983. Minimal model for membrane oscillations in the pancreatic β-cell. *Biophys. J.* 42:181–190.

Cook, D. L., and C. N. Hales. 1984. Intracellular ATP directly blocks K^+-channels in pancreatic β-cells. *Nature (Lond.).* 311:271–273.

Cook, D. L., M. Ikeuchi, and W. Y. Fujimoto. 1984. Lowering of pH inhibits calcium-activated potassium channels in isolated rat pancreatic islet cells. *Nature (Lond.).* 311:269–271.

Cook, D. L., L. S. Satin, M. L. J. Ashford, and C. N. Hales. 1988. ATP sensitive K^+ channels in pancreatic β-cells: Spare-channel hypothesis. *Diabetes.* 37:495–498.

Doedel, E. 1981. AUTO: A program for the automatic bifurcation analysis of autonomous systems. *Conq. Num.* 30:265–284.

Dunne, M. J., I. Findlay, O. H. Peterson, and C. B. Wollheim. 1986. ATP-sensitive K^+ channels in a insulin secreting line are inhibited by *d*-glyceraldehyde and activated by membrane permeabilization. *J. Membr. Biol.* 93:271–279.

Dunne, M. J., and O. H. Peterson. 1986. GTP and ADP activate ATP-inhibited K^+ channels in the insulin-secreting cell line RINm5F. *J. Physiol. (Lond.).* 381 67P.

Dunne, M. J., J. A. West-Jordan, R. J. Abraham, R. H. T. Edwards, and O. H. Petersen. 1988. The gating of nucleotide-sensitive K^+ channels in insulin-secreting cells can be modulated by changes in the ratio ATP^{4-}/ADP^{3-} and by nonhydrolyzable derivatives of both ATP and ADP. *J. Membr. Biol.* 104:165–177.

Fein, A., and M. Tsacopoulos. 1988. Activation of mitochondrial metabolism by calcium ions in *Limulus* ventral photoreceptors. Nature *(Lond.).* 331, 437–440.

Findlay, I., M. J. Dunne, and O. H. Peterson. 1985. High-conductance K^+ channel in pancreatic islet cells can be activated and inactivated by internal calcium. *J. Membr. Biol.* 83:169–175.

Himmel, D. M., and T. R. Chay. 1987. Theoretical studies on the electrical activity of pancreatic beta cells as a function of glucose. *Biophys. J.* 51:89–107.

Hindmarsh, A. C. 1974. Ordinary differential equation solver. Report UCID-30001. Lawrence Livermore Laboratory.

Kahaner, D., and D. Barnett. 1988. PLOD, version 4.9. National Bureau of Standards, Washington, DC.

Kakei, M., R. D. Kelly, S. Ashcroft, and F. Ashcroft. 1986. The ATP-sensitivity of K^+ channels in rat pancreatic B-cells is modulated by ADP. *FEBS (Fed. Eur. Biochem. Soc.) Lett.* 208:63–66.

Keizer, J. 1987. Statistical Thermodynamics of Nonequilibrium Processes. Springer-Verlag New York, Inc., NY. 135–138.

Keizer, J. 1988. Electrical activity and insulin release in pancreatic beta cells. *Math Biosci.* 90:127–138.

Malaisse, W., F. Malaisse-Lagae, and A. Sener. 1983. Anomeric specificity of hexose metabolism in pancreatic islets. *Physiol. Rev.* 63:773–786.

McDaniel, M., J. Colca, N. Kotagal, and P. Lacy. 1985. Regulation and role of intracellular Ca^{2+} in insulin secretion by the beta cell. *In* The Diabetic Pancreas. B. Volk and E. Arquilla, editors. Plenum Publishing Corp., New York. Chapt. 9.

Meissner, H. P. 1976. Electrical characteristics of the beta cells in pancreatic islets. *J. Physiol. (Paris).* 72:757–767.

Meissner, H. P., and I. Atwater. 1976. The kinetics of electrical activity of beta cells in response to a "square wave" stimulation with glucose or glibenclamide. *Horm. Metab. Res.* 8:11–16.

Misler, S., L. C. Falke, K. Gillis, and M. L. McDaniel. 1986. A metabolite-regulated potassium channel in rat pancreatic β-cells. *Proc. Natl. Acad. Sci. USA.* 83:7119–7123.

Nicholls, D. 1981. Some recent advances in mitochondrial calcium transport, *Trends Bio. Chem. Sci.* 6:36–38.

Ohno-Shosaku, T., B. J. Zünkler, and G. Trube. 1987. Dual effects of ATP on K^+ currents of mouse pancreatic beta cells. *Pluegers Arch. Eur. J. Physiol.* 408:133–138.

Plant, R. E. 1978. The effects of calcium on bursting neurons. *Biophys. J.* 21:217–237.

Plant, T. D. 1987. Calcium current inactivation in cultured mouse pancreatic islet cells is calcium-dependent. *J. Physiol. (Lond.).* 390:86 p.

Ribalet, B., and S. Ciani. 1987. Regulation by cell metabolism and adenine nucleotides of a K channel in insulin-secreting B cells (RIN m5F). *Proc. Natl. Acad. Sci. USA.* 84:1721–1725.

Rinzel, J. 1985. Bursting oscillations in an excitable membrane model. *In* Ordinary and Partial Differential Equations. B. D. Sleeman and R. J. Jarvis, editors. Springer-Verlag, New York, Inc., NY. 304–316.

Rinzel, J., T. R. Chay, D. Himmel, and I. Atwater. 1986. Prediction of the glucose-induced changes in membrane ionic permeability and cytosolic calcium by mathematical modeling. *In* Biophysics of Pancreatic Beta Cells. I. Atwater, E. Rojas, and B. Soria, editors. 247–263 pp.

Rinzel, J., and Y. -S. Lee. 1987. Dissection of a model for neuronal parabolic bursting. *J. Math. Biol.* 25:653–675.

Rorsman, P., H. Abrahamsson, E. Gylfe, and B. Hellman. 1984. Dual effects of glucose on the cytosolic Ca^{2+} activity of mouse pancreatic β-cells. *FEBS (Fed. Eur. Biochem. Sci.) Lett.* 170:196-200.

Rorsman, P., and G. Trube. 1986. Calcium and delayed potassium currents in mouse pancreatic β-cells under voltage clamp conditions. J. Physiol. *(Lond.).* 374:531–550.

Rubin, R. P. 1982. Calcium and Cellular Secretion. Plenum Publishing Corp., New York and London.

Sherman, A., J. Rinzel, and J. Keizer. 1988. Emergence of organized bursting in clusters of pancreatic beta cells by channel sharing. *Biophys. J.* 54:411–425.

Trube, G., P. Rorsman, and T. Ohno-Shosaku. 1986. Opposite effect of tolbutamide and diazoxide on the ATP-dependent K^+ channel in mouse pancreatic beta-cells. *Pluegers Arch. Eur. J. Physiol.* 407:493–499.

Wollheim, C. B., and G. W. G. Sharp. 1981. Regulation of insulin release by calcium. *Physiol. Rev.* 61:914–974.